Anharmonicity in single-wall carbon nanotubes as evidenced by means of extended energy loss fine structure spectroscopy analysis

P. Castrucci,[1] F. Tombolini,[1] M. Scarselli,[1] S. Bini,[1] M. De Crescenzi,[1] M. Diociaiuti,[2] S. Casciardi,[3]
M. A. El Khakani,[4,*] and F. Rosei[4]

[1]*Dipartimento di Fisica, Unità INFM, Università di Roma "Tor Vergata," Via della Ricerca Scientifica 1, 00133 Roma, Italy*
[2]*Dipartimento di Tecnologie e Salute, Istituto Superiore di Sanità, 00161 Roma, Italy*
[3]*Dipartimento di Igiene del Lavoro, ISPSEL, 00040 Monte Porzio Catone, Italy*
[4]*Institut National de la Recherche Scientifique, INRS-Énergie, Matériaux et Télécommunications 1650, Boulevard Lionel–Boulet,
Case Postale 1020, Varennes, Quebec J3X 1S2, Canada*

A comparative study of the structure of free-standing parallel bundles of single-wall carbon nanotubes (SWCNTs), multiwalled carbon nanotubes (MWCNTs), and highly oriented pyrolytic graphite (HOPG) was achieved by means of transmission electron microscopy and electron energy loss spectroscopy analyses. In particular, the carbon K ($1s$) extended fine structure of SWCNTs is found to be characterized by an apparent contraction of the nearest neighbors distance. This contraction is interpreted here to originate from an asymmetric pair distribution function, mostly due to the high out-of-plane vibrational motion of the C atoms, as for the case of chemisorbed atoms on clean surfaces. In contrast, the MWCNTs did not exhibit any signature of such an anharmonic effect because of their more rigid structure. This indicates that the SWCNTs pair potential is significantly broader and its effect is much weaker than that experienced by the same C-C pair embedded in a multiwall nanotube.

PACS number(s): 61.46.Fg, 61.10.Ht, 68.37.Lp

I. INTRODUCTION

It is well known that surface atoms experience an out-of-plane vibrational motion two or three orders of magnitude greater than the in-plane one.[1] This anharmonic effect is even enhanced in the case of adsorbates on clean surfaces.[2–7] Among structural techniques, surface extended x-ray absorption fine structure analysis is a powerful method to probe the strong anisotropy of the potential by extracting the structural parameters of the first neighbors shell.[8–10] Single wall carbon nanotubes (SWCNTs) consist of a rolled single sheet of carbon atoms, offering thereby a free-standing surface with two different modes of vibration (i.e., parallel and normal to the axis of the nanotube). Anharmonicity has been invoked as a possible interpretation for the observed temperature induced peak shifts [for the radial breathing modes (RBM) and G bands] in Raman spectra of SWCNTs.[11,12] However, it is to be noted that a Raman G-band shift (relatively lower than that of SWCNTs) has been also observed in multiwall carbon nanotubes (MWCNTs) (Ref. 13) and it is not clear yet if a comparable shift is present for highly oriented pyrolitic graphite (HOPG).[11–14] Thus, a clear evidence for the presence of anharmonicity in carbon nanostructures is still to be established.

In this paper, by achieving a comparative analysis of the fine structure of selected free-standing SWCNTs, MWCNTs, and HOPG, we were able to pinpoint the existence of anharmonic effects in SWCNTs induced by the large out-of-plane vibrations of their carbon atoms. Indeed, the Fourier transform, $F(R)$, of the extended-energy-loss fine structure (EXELFS) spectra revealed that the carbon atoms in SWCNT bundles undergo significant out-of-plane displacement. The $F(R)$ shows, in fact, an apparent reduction, as high as 11%, in the C-C first nearest neighbors distance with re-

spect to that obtained for MWCNTs and HOPG. These results can be interpreted in terms of the presence of an asymmetric radial distribution function, $g(r)$, due to the lack of atoms in the direction perpendicular to the SWCNT surface. In general, the asymmetry in the pair distribution function can be related to static and/or dynamic effects (i.e., structural disorder and thermal vibrations). However, in the present work, the observed asymmetry of $g(r)$ cannot be ascribed to the static disorder affecting the carbon nanotubes hexagonal network, because of the two following reasons: (i) the investigated carbon nanostructures were first examined under a transmission electron microscope and only defect-free and Co/Ni catalyst-free (as confirmed by electron energy loss spectroscopy) nanotubes were selected for the present EX-ELFS study; the objective being to investigate the intrinsic properties of carbon nanotubes; and (ii) it has been previously shown that no contraction of the C-C first coordination shell was observed even in the case of disordered amorphous carbon films.[15]

II. EXPERIMENTAL DETAILS

SWCNTs were synthesized by ablating a CoNi-doped graphite target, using a pulsed Nd:YAG laser in the superimposed double-pulse configuration.[16,17] MWCNTs were synthesized by arc discharge using two rods of natural graphite with a direct current flux of 80 A. Transmission electron microscopy (TEM) experiments were performed in a FEI TECNAI 12 (120 keV) apparatus equipped with an energy filter (GATAN GIF model) and a Peltier cooled SSC (slow scan charge-coupled device) multiscan camera (Model 794IR). The images were acquired before and after each electron energy loss spectroscopy (EELS) measurement to
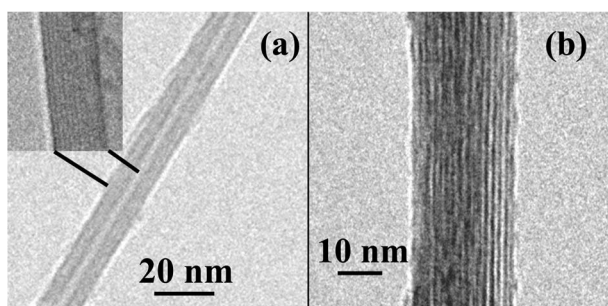
FIG. 1. Transmission electron micrographs of a 12 nm-diam. MWCNT (a) and a (22 ± 2) nm-diam. bundle of SWCNTs, of about 1.2 nm-diam. each (Ref. 20) (b). Since all the walls appear to be parallel and straight, the presence of structural defects (such as pentagons and heptagons) in the carbon hexagonal network can be considered to be negligible. In the inset we report a higher magnification of the TEM image of the inner walls of the MWCNT, showing a distance of about 0.37 nm between each graphene sheet.
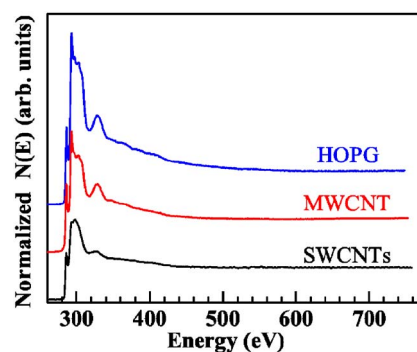

FIG. 2. (Color online) Electron energy loss spectra, after background subtraction, at the carbon K edges for HOPG, the MWCNT, and the SWCNTs rope. No nitrogen or oxygen K edge related features (at 409 and 530 eV, respectively) can be detected in all the three spectra.

ensure that the area under investigation had not suffered any morphological change and/or damage that may arise from the exposure to the high energy electron beam. While this procedure was successful on bundles of SWCNTs (down to ~5 nm-diam.), it does not permit us to acquire reliable data on individual tubes because of their damaging under extended exposure to the electron beam. Moreover, EELS was also used to ensure that no Ni/Co catalyst traces are present in the investigated carbon nanostructures. To this end, EELS spectra were systematically recorded, with a suitable energy range (i.e., 870–852 and 793–778 eV, respectively), to detect the eventual presence of any features of the Ni and Co $L_{2,3}$ edges (thus, one can detect the presence of Ni and Co atoms, if there is any, as long as they are not under the level of detectability of 1 atom over 10^4). The EXELFS spectra were acquired above the carbon K edge by probing the sample region selected in the image mode. A droplet of the raw synthesis product diluted in isopropyl alcohol was used to disperse the nanotubes on a gold TEM grid (mesh 1000). Several MWCNTs and bundles of parallel SWCNTs were found to be in a free-standing configuration (i.e., bridging adjacent grid wires). All the near-edge and extended energy loss measurements have been performed on free-standing tubes. For comparison purposes, similar experiments were also carried out on small flakes of HOPG, sufficiently thin not only to allow electron transmission but also to avoid multiple scattering processes inducing multiple losses that mask the genuine energy loss fine structures.

III. RESULTS AND DISCUSSION

Figures 1(a) and 1(b) display TEM images of a free-standing MWCNT and a free-standing bundle of parallelly packed SWCNTs, respectively. The diameter of the MWCNT is of ~12 nm, while that of the whole SWCNTs bundle is of (22 ± 2) nm (the diameter of a SWCNT is of ~1.2 nm, in accordance with the values deduced from Raman RBM analysis[17] and from STM measurements[18]). Particular care has been taken to record the electron energy loss spectra at

the carbon K edge only from the SWCNTs rope and from isolated MWCNTs, thus avoiding to collect electrons coming from any catalyst particles and/or carbonaceous products other than nanotubes. Moreover, the absence of any EELS signal at the $L_{2,3}$ edges of Ni and Co ensured us on the absence of catalyst atoms and clusters in the single wall carbon nanotubes cage. In addition, the SWCNTs bundle has been chosen to consist of parallelly packed and straight nanotubes in order to minimize the structural defects, such as pentagons and heptagons, in the hexagonal network of the investigated nanotubes. These structural defects, in fact, have been shown to produce coiled, bent, or twisted ropes of SWCNTs[19,20] and to induce different carbon K near edge signals.[20]

Figure 2 shows the collected spectral features due to the transition from the C 1s core level to p-like final unoccupied states.[21] The near edge signals (discussed in detail elsewhere[20]) show two prominent features: (i) the sharp peak near 286 eV, which is due to a transition from the 1s core level to the π^* band, and (ii) the structures in the 293–320 eV range, due to $1s \rightarrow \sigma^*$ transitions. The other features (above 320 eV) correspond to the scattering experienced by the 1s electrons in their final unoccupied states. They extend for several hundreds of eVs above the edge. In the limits of the dipole approximation, the nature of these features is very similar to that of the extended x-ray absorption fine structure (EXAFS) spectra obtained by using synchrotron radiation.[22,23] Therefore, EXELFS spectra can be analyzed with the same data procedure as for the EXAFS.[21] It is worth noting that no features of both N and O K edges (at 410 and 530 eV, respectively) can be detected in all these spectra. This is of paramount importance because nitrogen and/or oxygen can create structural defects in the nanotubes cage. Figures 3(a) and 3(b) show the EXELFS signals, $k\chi(k)$, after background subtraction and their corresponding Fourier transforms, $F(R)$, respectively. For the calculation of the $F(R)$ curves, a k-range extending from approximately k_{min} =4.4 Å^{-1} to k_{max}=11 Å^{-1} was used. Changes in the amplitude and phase can be clearly seen mainly for the SWCNTs sample compared to the HOPG. The $F(R)$ curves show three prominent peaks between 0.5 and 4.2 Å, corresponding to
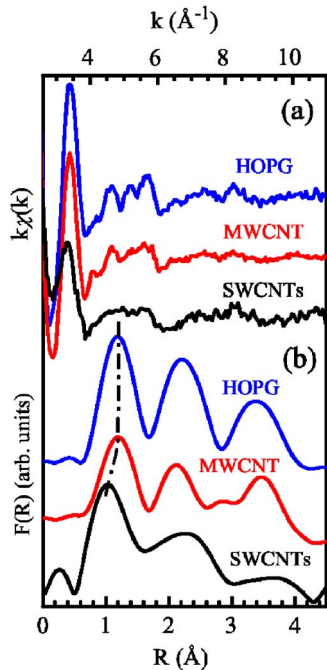
FIG. 3. (Color online) (a) EXELFS signals, $k\chi(k)$, and (b) their corresponding Fourier transforms, $F(R)$, for HOPG, a SWCNTs bundle, and a MWCNT. The k range for the $F(R)$ curve calculations is extended from approximately $k_{min}=4.4$ Å^{-1} to $k_{max}=11$ Å^{-1}.

the first nearest neighbors both in the basal plane and out-of-plane, in good agreement with the literature.[15,24,25] It is to be recalled here that the observed peak position in the $F(R)$ does not correspond exactly to the first neighbors distance of graphite (obtained through electron and x-ray diffraction experiments) because of the phase shift, $\phi_j(k)$, present in the EXAFS formula, that should be properly introduced to fit the $F(R)$.[22–24] Consequently, for example, the first nearest neighbor appears at 1.2 Å in the $F(R)$ instead of the 1.42 Å lattice atomic position value of graphite. A comparison of the $F(R)$ curves reveals a decrease of ~0.15 Å in the location of the first coordination shell for the SWCNTs with respect to those of either HOPG or MWCNT (this represents a C-C bond contraction of ~11%). However, such a C-C bond length contraction has been neither reported as a result of any electron diffraction measurement nor predicted by calculations of stability of carbon nanotubes with diameter greater than 1 nm.[26–28]

At this point, one should recall that carbon nanotubes may contain structural defects of which nature and density are highly dependent primarily on the used synthesis method (i.e., arc discharge, chemical vapor deposition (CVD), or laser ablation) and on its associated growth and purification conditions (e.g., temperature, pressure, catalysts, energy of the species,…). For example, the laser ablation method is known to grow SWCNTs with the highest purity,[17] whereas the highly energetic arc discharge process generally leads to relatively more defective nanotubes.[29] Moreover, it has been previously shown that no contraction of the C-C first coordination shell was observed even in the case of disordered amorphous carbon films.[15] As a consequence, given all the above discussed facts [i.e., cautious selection of free-

standing, straight, continuous parallely-packed, and defect-free samples, no detection of any electron-energy-loss spectroscopy (EELS) signal related to Co/Ni catalyst traces, and the absence of N and O contaminants], the observed important downshift of the first nearest neighbors shell cannot be ascribed to the presence of random distortions and/or structural defects in the SWCNT hexagonal network. On the other hand, an apparent contraction of the lattice parameter has been already observed by EXAFS (or EXELFS) in the case of low Z adsorbates.[4,6] This has been interpreted as a consequence of enhanced vibrations of the atoms giving rise to an anharmonic pair potential and an asymmetric pair distribution function, $g(r)$. Its observation in the present work is thought to be of the same origin and bound to be enhanced out-of-plane vibrations of the C atoms of SWCNTs. In fact, this anharmonicity enters in the EXAFS formalism originally derived by Stern et al.[22] For systems with pair distribution function that deviates from a Gaussian shape, the cumulant expansion approach introduced by Bunker[30] is often used and the phase function, for a given j shell, in the EXAFS-EXELFS equation becomes

$$\psi_j(k) = 2k\mathrm{R}_j + \phi_j(k) - 4/3\mathrm{C}_{3j}k^3 + \mathrm{O}(k^5), \qquad (1)$$

where ϕ_j is the phase shift. C_{3j} is a measure of the deviation of the pair distribution function from a Gaussian shape centred at R_j (i.e., the distance between the absorbing and scattering atoms). The C_{3j} value enters in the $g(r)$ expression through the pair potential $U(r)$, which can be expressed as follows (by assuming, for example, a Morse form):[8,9,31–33]

$$U(r) = D\{e^{-2\alpha(r-R_j)} - 2e^{-\alpha(r-R_j)}\}, \qquad (2)$$

where α is a function of C_{3j} and D is the well depth. The pair potential $U(r)$ is related to the radial distribution function, $g(r)$, through the following expression:

$$g(r) = e^{-U(r)/kT}. \qquad (3)$$

If the radial movement of atoms is particularly large, $g(r)$ is expected to be highly asymmetric. In contrast, $g(r)$ can be approximated to a Gaussian function in the case of thermal isotropic disorder.

The asymmetry of $g(r)$, resulting from the out-of-plane motion of the C atoms, leads to an apparent shortening in the $F(R)$.

To point up the anharmonic effect in SWCNTs, we extracted the contribution $\chi_1(k)$ and $\psi_1(k)$ of the first neighbor shell starting from the Fourier filtered curves of Fig. 3(b). Thus, the EXELFS signals, $k\chi_1(k)$, for HOPG, SWCNTs, and MWCNT are shown in Fig. 4. Compared to HOPG, the MWCNT-$k\chi_1(k)$ curve shows an amplitude reduction and a similar oscillation frequency with k. The general accordance between the two curves suggests that carbon atoms are experiencing a similar thermal motion in either HOPG or MWCNT structures. On the other hand, the $k\chi_1(k)$ curve of the SWCNTs is found to present a higher amplitude reduction, especially at high k values, with respect to the HOPG curve (Fig. 4), suggesting that the thermal motion for C atoms is much higher in SWCNTs than in graphite. This is confirmed by the $k\chi_1(k)$ oscillation frequency of SWCNTs
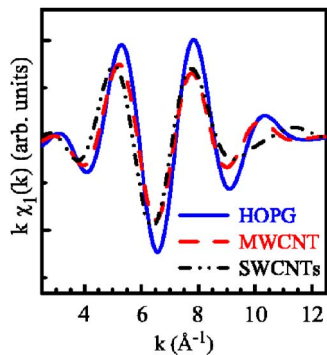
FIG. 4. (Color online) EXELFS signal $k\chi_1(k)$ only from nearest-neighbor shell after Fourier filtering (approximately from R_{min} =0.5 Å to R_{max}=1.7 Å) for HOPG (solid line), a SWCNTs bundle (dot-dashed line), and a MWCNT (dashed line).

which is different from that of HOPG. This can be better seen by plotting the phase difference $\Delta\psi$ between the HOPG and the two nanotube types (i.e., MWNTs and SWCNTs) as a function of k [Fig. 5(a), circles and triangles curves]. This comparison is justified by the complete transferability of the amplitude and phase shift for the C-C pairs in different materials.[34] These curves have been fitted by a fifth degree k odd function

$$\Delta\psi(\text{CNT, HOPG}) = \psi_1(\text{CNT}) - \psi_1(\text{HOPG})$$
$$= 2\Delta R k - 4/3\Delta C_3 k^3 + O(k^5). \quad (4)$$

The fifth order terms are found to be less than 10^{-5} Å^{-5} in the case of MWCNTs and zero for the SWCNTs bundle. The ΔR values obtained from the fit, approximately of the order
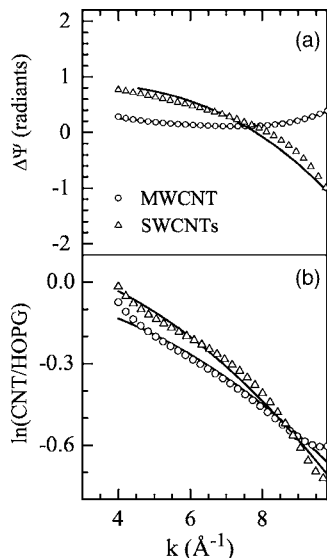

FIG. 5. (a) Phase difference of the EXELFS signal $k\chi_1(k)$, only from nearest-neighbor shell, between HOPG and both types of nanotubes [MWCNTs (circles) and SWCNTs rope (triangles), respectively]. (b) Logarithmic ratio of the backscattering amplitude of SWCNTs rope versus HOPG (triangles) and MWCNTs versus HOPG (circles). The solid curves represent the best fit to the experimental data.

TABLE I. Best fit results for the deviation of the pair distribution function (ΔC_3) from a Gaussian shape centered at the first nearest neighbor R_1 for both SWCNTs and MWCNTs with respect to that of HOPG. ΔC_2 is the mean square relative displacement between the absorber and the first nearest neighbors backscatterer for SWCNTs and MWCNTs with respect to the HOPG reference.

	$\Delta C_3 (\times 10^{-3}$ Å$^3)$	$\Delta C_2 (\times 10^{-3}$ Å$^2)$
SWNTs	1.9±0.3	4.2±0.3
MWNT	0.3±0.2	3.3±0.3

of 10^{-2} Å, indicate that no real shrinking of the first neighbors distance is to be considered within the experimental errors for both types of nanotubes. This means that there is no sizeable difference between the first neighbor distance of SWCNTs, MWCNTs, and HOPG. On the other hand, the ΔC_3 values, reported in Table I, show that SWCNTs exhibit a ΔC_3 value about six times larger than that quoted for MWCNTs. To have found nonzero ΔC_3 values means that the harmonic approximation is not sufficient to describe the C-C relative motion in both cases, but the great difference between the two ΔC_3 values is a clear hint of the high anharmonicity experienced by the C-C pairs in SWCNTs.

An additional confirmation of the stronger motion of the C atoms in the SWCNTs (in comparison with the MWCNTs) can be derived from the analysis of the logarithmic ratio of the amplitudes $A_1(k)$ of the $\chi_1(k)$ between the HOPG and both types of nanotubes (i.e., SWCNTs and MWCNTs). This logarithmic ratio is directly related to the second cumulant ΔC_2 according to the following equation:[30]

$$\ln[A_1(\text{CNT})/A_1(\text{HOPG})] = -2\Delta C_2 k^2 + O(k^4), \quad (5)$$

where ΔC_2 represents the mean-square relative displacement between the absorber and the back scatterer (i.e., the EXAFS-EXELFS Debye-Waller factor equivalent in the harmonic approximation) and is related to the width of the pair distribution function. The measured behaviors and their related least squared fits are shown in Fig. 5(b). The ΔC_2 values obtained from the best fit [solid lines of Fig. 5(b)] of the experimental data are reported in Table I. The ΔC_2 of SWCNTs is found to be about 30% higher than that of the MWCNTs. This indicates that the magnitude of the thermal motion of C atoms in the SWCNTs grouped in bundles is much larger than in the MWCNTs, in accordance with the above discussed results. These quantitative results constitute a clear evidence for the occurrence of anharmonicity in SWCNTs. A considerable reduction of the number of nanotubes in the rope has been found to not affect the reported apparent contraction. Indeed, the $F(R)$ of both 5 nm-diam. and 20 nm-diam. SWCNT bundles (corresponding approximately to 4 and 15 tubes along the bundle radial direction, respectively) were found to be fairly identical (the first neighbor is located at the same radial position for both bundles). This suggests that a considerable reduction of the number of nanotubes in the bundle does not affect the reported apparent contraction. In other words, the radial motion of the C atoms in SWCNTs seems to not be affected by

the presence of other tubes in the bundle. Very different is the case of MWCNTs where the structure is rather stiff and the atoms have less freedom of movement because of the presence of neighboring atomic layers from each side. [This corroborates well with the much smaller effect in the $g(r)$ asymmetry that was observed for MWCNTs.] Finally, our findings also bring a solid argument for the previously invoked possibility of anharmonicity to explain the relatively larger temperature-induced shift in the Raman vibrations modes of SWCNTs (in comparison with MWCNTs).[11–13]

IV. CONCLUSIONS

In conclusion, we evidenced that the carbon atoms in a single wall tubes are affected by an out-of-plane thermal motion greater than in MWCNTs or in HOPG structures. Since the investigated nanotubes were carefully selected to minimize strongly (to not to say to eliminate) the static effects, the reported effects are interpreted to be due to the anharmonicity of the C-C pair potential in SWCNTs. Very interesting

would be to study the EXELFS behavior of carbon nanotubes with structural defects, such as opened holes in the hexagonal cage for N incorporation or the presence of metal catalyst particles which should reduce or completely hamper the movement of carbon atoms. This, in turn, may also help in improving our understanding of the origin of the high surface reactivity to a foreign agent of the SWCNTs with respect to the other carbon systems. Future work will be aimed at investigating the effect of anharmonicity on organic molecules and polymers adsorbed on SWCNTs, to better understand the adsorption mechanism. This could also help to elucidate the much higher efficiency in photovoltaic conversion demonstrated by these composites as opposed to SWCNTs.[35]

ACKNOWLEDGMENTS

*Corresponding author. Electronic address: elkhakani@emt.inrs.ca

[1] J. B. Pendry, *Low Energy Electron Diffraction* (Academic Press, Inc., London, 1974).

[2] G. M. Lamble, R. S. Brooks, S. Ferrer, D. A. King, and D. Norman, Phys. Rev. B **34**, 2975 (1986).

[3] P. Roubin, D. Chandesris, G. Rossi, J. Lecante, M. C. Desjonqueres, and G. Treglia, Phys. Rev. Lett. **56**, 1272 (1986).

[4] L. Wenzel, J. Stöhr, D. Arvanitis, and K. Baberschke, Phys. Rev. Lett. **60**, 2327 (1988).

[5] R. Franchy, M. Wuttig, and H. Ibach, Surf. Sci. **203**, 489 (1988).

[6] L. Wenzel, D. Arvanitis, H. Rabus, T. Lederer, K. Baberschke, and G. Comelli, Phys. Rev. Lett. **64**, 1765 (1990).

[7] H. Wende, D. Arvanitis, M. Tischer, R. Chauvistre, H. Henneken, F. May, and K. Baberschke, Phys. Rev. B **54**, 5920 (1996).

[8] P. Eisenberger and G. S. Brown, Solid State Commun. **29**, 481 (1979).

[9] M. De Crescenzi, F. Antonangeli, C. Bellini, and R. Rosei, Solid State Commun. **46**, 875 (1983).

[10] J. M. Tranquada, in *EXAFS and Near Edge Structure III*, edited by K. O. Hodgson, B. Hedman, and J. E. Penner-Hahn, Springer Proceedings in Physics Vol. 2 (Springer-Verlag, Berlin, 1984), p. 74.

[11] P. V. Huong, R. Cavagnat, P. M. Ajayan, and O. Stephan, Phys. Rev. B **51**, 10048 (1995).

[12] H. D. Li, K. T. Yue, Z. L. Lian, Y. Zhan, L. X. Zhou, S. L. Zhang, Z. J. Shi, Z. N. Gu, B. B. Liu, R. S. Yang, H. B. Yang, G. T. Zou, Y. Zhang, and S. Iijima, Appl. Phys. Lett. **76**, 2053 (2000), and references therein.

[13] F. M. Huang, K. T. Yue, P. H. Tan, S. L. Zhang, Z. J. Shi, X. H. Zhou, and Z. N. Gu, J. Appl. Phys. **84**, 4022 (1998).

[14] P. Tan, Y. Deng, Q. Zhao, and W. Cheng, Appl. Phys. Lett. **74**, 1818 (1999).

[15] G. Comelli, J. Stöhr, C. J. Robinson, and W. Jark, Phys. Rev. B **38**, 7511 (1988).

[16] The target, placed in a quartz tube at the center of a furnace, was ablated with a laser intensity of $\sim 2.5 \times 10^9$ W/cm^2, at $T = 1150\ °C$ in a flowing Ar gas. The synthesis product was collected on a water-cooled surface at the furnace exit. More details are reported in Ref. 17.

[17] N. Braidy, M. A. El Khakani, and G. A. Botton, Carbon **40**, 2835 (2002).

[18] P. Castrucci, M. Scarselli, M. De Crescenzi, M. A. El Khakani, F. Rosei, N. Braidy, and J. H. Li, Appl. Phys. Lett. **85**, 3857 (2004).

[19] S. Ihara, S. Itoh, and J. Kitakami, Phys. Rev. B **48**, 5643 (1993).

[20] P. Castrucci, M. De Crescenzi, M. Scarselli, M. Diociaiuti, P. Chistolini, M. A. El Khakani, and F. Rosei, Appl. Phys. Lett. **87**, 103106 (2005).

[21] EELS probes unoccupied electron states above the Fermi level in the energy range of core edge levels. It yields information similar to that provided by x-ray absorption spectroscopy, assuming that the dipole transition selection rule dominates the matrix element of the scattering process. More details can be found in M. De Crescenzi, Surf. Sci. Rep., **21**, 89 (1995).

[22] E. A. Stern, D. E. Sayers, and F. W. Lytle, Phys. Rev. B **11**, 4836 (1975).

[23] S. M. Heald and E. A. Stern, Phys. Rev. B **17**, 4069 (1978).

[24] B. M. Kincaid, A. E. Meixner, and P. M. Platzman, Phys. Rev. Lett. **40**, 1296 (1978).

[25] M. M. Disko, O. L. Krivanek, and P. Rez, Phys. Rev. B **25**, 4252 (1982).

[26] Ph. Lambin, V. Meunier, L. Henrard, and A. A. Lucas, Carbon **38**, 1713 (2000).

[27] K. Hirahara, S. Bandow, H. Kataura, M. Kociak, and S. Iijima, Phys. Rev. B **70**, 205422 (2004).

[28] Z. Peralta-Inga, S. Boyd, J. S. Murray, C. J. O'Connor, and P. Politzer, Struct. Chem. **14**, 431 (2003).

[29] M. Monthioux, B. W. Smith, B. Burteaux, A. Claye, J. E. Fisher,

and D. E. Luzzi, Carbon **39**, 1251 (2001).

[30] G. Bunker, Nucl. Instrum. Methods Phys. Res. **207**, 437 (1983).

[31] D. P. Jackson, Surf. Sci. **43**, 431 (1974).

[32] L. A. Girifalco and V. G. Weizer, Phys. Rev. **114**, 687 (1959).

[33] J. R. Xiao, B. A. Gama, and J. W. Gillespie, Jr., Int. J. Solids Struct. **42**, 3075 (2005); and references therein.

[34] P. A. Lee, P. H. Citrin, P. Eisenberger, and B. M. Kincaid, Rev. Mod. Phys. **53**, 769 (1981).

[35] D. M. Guldi, G. M. A. Rahman, F. Zerbetto, and M. Prato, Acc. Chem. Res. **38**, 871 (2005).